JOURNAL OF SOLID STATE CHEMISTRY 63, 377–385 (1986)

Tc_2P_3 with Tc_2As_3-type Structure and Structure Refinement of Mo_2As_3

L. H. DIETRICH AND W. JEITSCHKO

Anorganisch-Chemisches Institut, Universität Münster, Corrensstr. 36, D-4400 Münster, West Germany

Received September 25, 1985

A previously reported technetium phosphide has the composition Tc_2P_3 and crystallizes in the triclinic space group $P\bar{1}$ with the lattice constants $a = 6.266(1)$ Å, $b = 6.325(1)$ Å, $c = 7.683(2)$ Å, $\alpha = 95.79(1)°$, $\beta = 101.76(1)°$, $\gamma = 104.34(1)°$, $V = 285.1(2)$ Å^3. Its crystal structure was determined from X-ray data of a twinned crystal and refined to a residual of $R = 0.035$ for 1790 structure factors and 92 variable parameters. Tc_2P_3 is isotypic with Tc_2As_3, which has a superstructure of Mo_2As_3. The structure of Mo_2As_3 is confirmed. It was refined from single-crystal counter data to a residual of $R = 0.031$ (893 F values, 17 variables). A comparison of the structures of Tc_2P_3 and Tc_2As_3 reveals a tendency towards more localized bonding in the structure of Tc_2P_3. The twinning and the anisotropic thermal parameters of Tc_2P_3 are discussed within the context of a potential displacive phase transition of this compound at higher temperatures.

Introduction

The first and only investigation of the system technetium-phosphorus resulted in the identification of six compounds (*1*). At that time only those with the lowest and highest phosphorus content were found to be isotypic with known manganese or rhenium phosphides: Tc_3P has the Mn_3P (Fe_3P type) structure and TcP_4 is isotypic with ReP_4 (*1*). Later on the structure determination of TcP_3 resulted in a new structure type which was also found for ReP_3 (*2*). In the present investigation we report the crystal structure of Tc_2P_3. This compound has been identified as "Phase C" previously (*1*). Tc_2P_3 is isotypic with Tc_2As_3 (*3*) which has a superstructure of Mo_2As_3 caused by differences in metal–metal bonding. The structure of Mo_2As_3 had been determined originally from single-crystal film data (*4*). For comparison we have now reinvestigated and refined this structure from single-crystal counter data.

Crystal Structure of Tc_2P_3

Tiny crystals and Guinier powder patterns of the technetium phosphide "Phase C" (*1*) were kindly provided by Dr. R. Rühl. The crystals had been obtained from a sample prepared by the tin-flux technique with the starting composition Tc : P : Sn = 1 : 3 : 6 as described previously (*1*).

Because of the superstructure and the strong tendency for twinning, the true symmetry of the Tc_2P_3 crystals was not immediately recognized. Buerger and Weissenberg diffractograms recorded with Mo$K\alpha$ radiation revealed a very pronounced centered monoclinic subcell, which eventually was recognized as corresponding to the struc-

0022-4596/86 $3.00

TABLE I

GUINIER POWDER PATTERN OF Tc_2P_3[a]

h	k	l	Q_o	Q_c	I_o	I_c	h	k	l	Q_o	Q_c	I_o	I_c
0	0	1	182	181	vw	3	0	1	3	2119	2119	s	59
0	1	0	274	273	w	5	2	1	1	2202	2201	s	20
1	0	−1	—	361	—	2	2	−2	−2		2202		20
0	1	−1	384	384	vs	100	0	2	−3	2302	2299	s	37
0	1	1	527	526	s	37	2	0	2	2312	2309	s	36
0	0	2	727	725	w	5	2	−1	−3		2310		37
0	1	−2	858	857	vs	70	*3	−1	0	2398	2398	vw	3
0	2	0	1094	1093	vw	4	0	3	−1	2427	2427	vw	7
2	−1	0	1115	1115	m	7	0	3	0	2461	2459	m	27
2	0	−1		1115		6	2	−2	2	2503	2500	m	16
0	2	−1	1132	1132	m	34	2	1	−3		2501		17
0	1	2	1142	1141	m	32	2	−3	0	2682	2683	vs	61
2	0	0	1152	1150	s	27	2	2	−1		2683		60
2	−1	−1		1150		26	0	3	−2	2759	2758	s	34
0	2	1	1418	1416	s	34	2	2	0	2861	2860	vw	2
2	−1	1	1444	1442	vs	46	2	−3	−1		2861		2
2	0	−2		1442		48	0	0	4	2903	2902	vs	43
0	2	−2	1535	1534	w	12	2	1	2	3030	3033	m	16
2	0	1	1549	1548	m	12	2	−2	−3		3034		16
2	−1	−2		1549		11	0	3	−3	3453	3452	w	13
2	−2	0	1626	1626	w	2	0	1	4	—	3459	—	6
2	1	−1		1626		2	2	−2	3	3482	3482	s	47
0	0	3	1633	1632	m	11	2	1	−4		3483		48
0	1	−3	1694	1692	m	16	0	3	2	3610	3611	m	23
2	1	0	1733	1732	vs	69	*3	−3	−1	3729	3727	vw	1
2	−2	−1		1732		71	*3	−2	2	3843	3846	vw	2
2	−2	1	1881	1881	m	7	4	−1	−1	4073	4075	s	49
2	1	−2		1882		8							

[a] The pattern was recorded with Cu$K\alpha_1$ radiation. The Q values are defined by $Q = 10^4/d^2$ (Å^{-2}). For the calculation of the intensities (*5*) the positional parameters of the single-crystal refinement were used. The line splitting due to the triclinic distortion of the (pseudo-)monoclinic subcell is too small to be observable; however, three weak superstructure reflections (marked with asterics) caused by the doubling of the (pseudo-)monoclinic *b* axis indicate the lower symmetry also in the powder pattern. Because of the large number of calculated reflections only all observed and those with calculated intensitics $I_c > 2$ are listed.

ture of Mo_2As_3 and W_2As_3 (*4*). Lattice constants for this cell were refined from the Guinier powder data using α-quartz (a = 4.9130 Å, c = 5.4046 Å) as standard. In the standard $C2/m$ setting of this cell the lattice constants are a = 12.256(2) Å, b = 3.133(1) Å, c = 8.912(2) Å, β = 123.57(1)°, V = 285.1(2) Å^3. The structure determination with this cell, however, resulted in large thermal amplitudes for the Tc atoms in the direction of the (pseudo-)monoclinic *b* axis. This suggested to us the possibility of a doubling of this axis in the true cell. A systematic search for superstructure reflections on a four-circle diffractometer confirmed this suspicion, although these reflections are so weak that they could not be observed on the corresponding heavily exposed cone axis diffractograms.

At this stage we had succeeded with the structure determination of Tc_2As_3 (*3*) which was carried out at the same time. The isotypy of the two compounds was proven by the structure refinement of Tc_2P_3. Thus the true symmetry of Tc_2P_3 is triclinic with the following lattice constants obtained from a

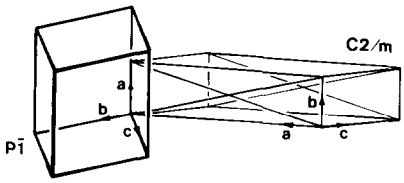

FIG. 1. Relation of the triclinic cell of the superstructure of Tc_2P_3 to the monoclinic Mo_2As_3 type subcell in the *C2/m* standard setting.

careful evaluation of the Guinier powder data (Table I): $a = 6.266(1)$ Å, $b = 6.325(1)$ Å, $c = 7.683(2)$ Å, $\alpha = 95.79(1)°$, $\beta = 101.76(1)°$, $\gamma = 104.34(1)°$, $V = 285.1(2)$ Å^3. The transformation matrix from the monoclinc subcell in the *C2/m* standard setting to the triclinic cell of the superstructure is $0,2,0/\frac{1}{2},-\frac{1}{2},0/-\frac{1}{2},-\frac{1}{2},-1$ (Fig. 1).

An additional problem which complicated the structure determination was the twinning. All eleven crystals of Tc_2P_3 examined in the Buerger cameras turned out to be twinned with the reciprocal lattice points $0kl$ of the monoclinic subcell of one twin orientation coinciding with the lattice points $0\bar{k}\bar{l}$ of the other twin orientation. For $h = \pm 2$, reflections of the one twin orientation violate the *C* centering extinction condition of the subcell of the other twin orientation, and for $h = \pm 4$ the two reciprocal lattices nearly overlap; however, fortunately for higher orders of h the two reciprocal lattices become more resolved and can be observed separately. Laue symmetry *mmm* is mimicked if the scattering from both twins is about equal.

The crystal used for the collection of the intensity data on a four-circle diffractometer had the extensions $30 \times 30 \times 40$ μm^3. Its two twin orientations had an intensity ratio of about 1 : 5 for equivalent reciprocal lattice points and only the more intense reciprocal lattice was recorded with $\theta/2\theta$ scans, graphite monochromated Mo$K\alpha$ radiation, a scintillation counter, and a pulse-height discriminator. Background counts were taken at both ends of each scan; the scan speed was optimized by a fast prescan. An empirical absorption correction was applied from psi-scan data (linear absorption coefficient $\mu_{MoK\alpha} = 108.3$ cm^{-1}). The ratio of the maximal to the minimal transmission was 1.14. A total of 9414 reflections (including the superstructure reflections which were overlooked at first) was measured in the whole reciprocal space up to $2\theta = 90°$. Equivalent reflections were averaged, reflections of the twins which were superimposed and reflections with $F_0 < 4\sigma(F_0)$ were omitted.

The structure of the very pronounced monoclinic *C* centered subcell was solved first. The cell content of Tc_8P_{12} was obtained from a plot of average atomic volumes in the Tc–P and Re–P systems. This corresponds to an X-ray density of 6.73 g · cm^{-3}. The Patterson projection could be partially interpreted considering crystal chemical arguments; the remaining atoms were located on difference Fourier plots. The structure was refined by full-matrix least-squares calculations using scattering factors for neutral atoms (*6*), corrected for anomalous dispersion (*7*). Weights were assigned according to counting statistics. A secondary extinction parameter was refined and applied to the calculated structure factors. The conventional residual for this refinement of the subcell with isotropic thermal parameters was $R = 0.101$ for 890 structure factors and 17 variable parameters (Table II). This subcell corresponds to the structure of Mo_2As_3 (*4*).

A refinement with anisotropic thermal parameters of this subcell reduced the residual to $R = 0.045$. A comparison of the two refinements showed that the thermal amplitudes of the phosphorus atoms did not differ very much, while the ellipsoids of the Tc atoms were cigar-shaped with great thermal amplitudes perpendicular to the mirror plane of the subcell. The subcell was then refined with poor results in various

TABLE II

ATOM PARAMETERS OF Mo_2As_3 AND OF THE SUBCELL OF Tc_2P_3[a]

Compound	Atom	x	z	B[Å²]
Mo_2As_3	Mo(1)	0.24801(4)	0.37127(7)	0.264(6)
(This work)	Mo(2)	0.35103(4)	0.13539(7)	0.274(6)
	As(1)	0.12674(5)	0.04751(9)	0.384(9)
	As(2)	0.41512(5)	0.68540(9)	0.346(9)
	As(3)	0.10383(5)	0.62754(9)	0.324(9)
Mo_2As_3 (*4*)	Mo(1)	0.2482(4)	0.3712(7)	1.1(1)
	Mo(2)	0.3511(4)	0.1355(7)	1.2(1)
	As(1)	0.1270(6)	0.0471(10)	1.3(2)
	As(2)	0.4145(6)	0.6855(10)	1.4(2)
	As(3)	0.1035(6)	0.6275(10)	1.2(2)
Tc_2P_3 (Subcell)	Tc(1)	0.2499(1)	0.3653(1)	0.69(1)
	Tc(2)	0.3632(1)	0.1424(1)	0.38(1)
	P(1)	0.1099(3)	0.0403(3)	0.33(4)
	P(2)	0.4116(3)	0.6797(3)	0.35(4)
	P(3)	0.0985(3)	0.6274(3)	0.56(4)

[a] For comparison the parameters obtained by Jensen *et al.* (*4*) are listed after transformation to the standard setting of the *C2/m* cell. All atoms are in position (4i) *x*, 0, *z* of this space group. The standard deviations of the least significant digits are given in parentheses.

lower symmetry space groups until the structure of Tc_2As_3 (*3*) was solved and the potential isotypy of Tc_2P_3 with Tc_2As_3 was recognized. A refinement of the Tc_2P_3 subcell data in the triclinic cell corresponding to that of Tc_2As_3 immediately gave satisfactory thermal amplitudes for all atoms. The *R* value was 0.049 for a refinement with isotropic thermal parameters, 42 variables, and 1093 structure factors.

The data were now remeasured to include the superstructure reflections. The full-matrix least-squares refinement of this data set confirmed the isotypy of Tc_2P_3 and Tc_2As_3. The residual for a refinement with isotropic thermal parameters was $R = 0.049$. The final residual for the refinement with ellipsoidal thermal parameters, 92 variables, and 1790 *F* values is $R = 0.035$. A final difference Fourier synthesis showed no electron density values higher than 2.1 e/Å³. Positional and anisotropic thermal parameters are listed in Tables III and IV, interatomic distances in Table V. The structure is shown in Fig. 2. A listing of the structure factors is available from the authors.

TABLE III

ATOM PARAMETERS OF Tc_2P_3[a]

Atom	x	y	z	B(Å²)
Tc(1)	0.92338(8)	0.13096(8)	0.63174(7)	0.293(7)
Tc(2)	0.46119(8)	0.13780(9)	0.63769(7)	0.303(7)
Tc(3)	0.61995(8)	0.58315(8)	0.85986(7)	0.227(6)
Tc(4)	0.09992(8)	0.58510(9)	0.85520(7)	0.244(7)
P(1)	0.5373(3)	0.1828(3)	0.9622(3)	0.32(2)
P(2)	0.0328(3)	0.1771(3)	0.9563(3)	0.31(2)
P(3)	0.6297(3)	0.8494(3)	0.6785(3)	0.34(2)
P(4)	0.1378(3)	0.8643(3)	0.6815(3)	0.28(2)
P(5)	0.7650(3)	0.4375(3)	0.6189(2)	0.32(2)
P(6)	0.2644(3)	0.4231(3)	0.6364(2)	0.34(2)

[a] All atoms are in the general position of space group $P\bar{1}$. Standard deviations in the least significant digit are given in parentheses. The last column contains isotropic thermal parameters as obtained in a previous refinement of the structure.

Structure Refinement of Mo_2As_3

Because of the close resemblance of the structures of Tc_2P_3 and Tc_2As_3 to that of Mo_2As_3 we considered it worthwhile to reexamine the structure of the latter compound. After all the subcells of Tc_2P_3 and

TABLE IV

THERMAL ELLIPSOIDS IN THE STRUCTURE OF Tc_2P_3[a]

Atom	U_{11}	U_{22}	U_{33}	U_{12}	U_{13}	U_{23}
Tc(1)	54(1)	24(2)	22(2)	4(1)	5(1)	5(1)
Tc(2)	54(1)	23(2)	25(2)	2(1)	1(1)	4(1)
Tc(3)	41(1)	19(1)	21(1)	6(1)	1(1)	0(1)
Tc(4)	42(1)	25(1)	23(1)	9(1)	2(1)	3(1)
P(1)	43(4)	37(5)	34(5)	8(4)	0(4)	0(4)
P(2)	44(4)	27(5)	39(5)	6(4)	8(4)	−7(4)
P(3)	45(4)	42(5)	40(5)	17(4)	11(4)	17(4)
P(4)	38(4)	52(5)	36(5)	18(4)	5(4)	17(4)
P(5)	47(4)	41(5)	34(5)	12(4)	7(4)	12(4)
P(6)	40(4)	58(6)	37(5)	11(4)	11(4)	−3(5)

[a] The parameters are multiplied by 10^4; they are listed in the form $\exp[-2\pi^2(h^2a^{*2}U_{11} + \cdots + 2hka^*b^*U_{12} + \cdots)]$.

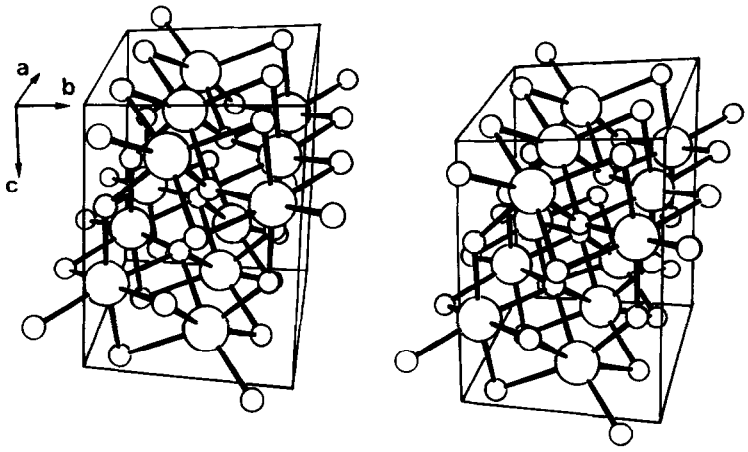

FIG. 2. Stereoplot of the structure of Tc_2P_3. Outlined is the triclinic cell of the superstructure. Large spheres: Tc; small spheres: P. Only the Tc–P bonds are indicated.

Tc_2As_3 correspond to the structure of Mo_2As_3 which was refined only from film data (*4*) and we had recognized the superstructure of Tc_2P_3 only by the unusual anisotropic thermal parameters of the Tc atoms.

Samples of Mo_2As_3 were prepared by reaction of powders of the elemental components in silica tubes as described previously (*8–10*). The Guinier powder patterns were indexed and refined on the basis of the monoclinic *C2/m* cell in the standard setting: a = 13.361(1) Å, b = 3.2337(3) Å, c = 9.6385(5) Å, β = 124.57(4)°, V = 342.9(1) Å^3. These lattice constants correspond to a = 16.057(1) Å, b = 3.2337(3) Å, c = 9.6385(5) Å, β = 136.75(4)° in the setting of Jensen *et al.* (*4*). They are in reasonable agreement with those reported before: 13.339(2), 3.240(2), 9.628(2) Å, 124.52(3)° in the standard setting given by Taylor *et al.* (*10*) and 16.061(2), 3.2349(4), 9.643(1) Å, 136.74(2)° in the setting of Jensen *et al.* (*4*).

Single crystals of Mo_2As_3 were investigated in a four-circle diffractometer. They did not reveal any superstructure reflections corresponding to the triclinic cell of Tc_2As_3. For the structure refinement a data set of 5648 reflections was collected under the experimental conditions outlined above for Tc_2P_3, for the monoclinic cell of a crystal with a diameter varying between 30 and 40 μm. An absorption correction from psi-scan data correspond to a ratio of maximal to minimal transmission of 1.34 (calculated density ρ_c = 8.06 g · cm^{-3}, linear absorption coefficient $\mu_{MoK\alpha}$ = 355 cm^{-1}). After averaging of equivalent data and omitting reflections with counting statistics less than three standard deviations, 893 structure factors remained which were used for a structure refinement as described above. The final residual is R = 0.031 for a refinement with isotropic thermal parameters and 17 variable parameters (Table II). Interatomic distances are listed in Table V. A refinement with anisotropic thermal parameters lowered the residual to only R = 0.030 (32 variables). None of the thermal ellipsoids differed greatly from a sphere.

Discussion

Tc_2P_3 is isotypic with Tc_2As_3 whose structure was discussed before (*3*). The structure is intermediate between those of transition metal phosphides with high coordination number for all atoms, as is typical

TABLE V

INTERATOMIC DISTANCES (Å) IN Tc_2P_3 AND Mo_2As_3[a]

Tc(1):	P(3)	2.337	Tc(2):	P(4)	2.423	Mo(1):	As(2)	2.512
	P(4)	2.363		P(3)	2.394		As(2)	2.546
	P(5)	2.389		P(6)	2.424		As(3)	2.551
	P(2)	2.415		P(1)	2.414		As(1)	2.574
	P(4)	2.416		P(3)	2.340		As(2)	2.512
	P(6)	2.446		P(5)	2.370		As(3)	2.551
	Tc(2)	2.865		Tc(1)	2.865		Mo(1)	2.937
	Tc(2)	2.917		Tc(1)	2.917		Mo(1)	3.234
	Tc(1)	2.944		Tc(2)	2.801		Mo(1)	2.937
	Tc(4)	3.013		Tc(3)	2.964		Mo(2)	3.258
	Tc(2)	3.350		Tc(1)	3.350		Mo(1)	3.234
Tc(3):	P(3)	2.289	Tc(4):	P(4)	2.314	Mo(2):	As(2)	2.573
	P(2)	2.389		P(1)	2.434		As(1)	2.531
	P(5)	2.420		P(6)	2.412		As(3)	2.576
	P(1)	2.428		P(2)	2.392		As(1)	2.531
	P(6)	2.431		P(5)	2.389		As(3)	2.576
	P(1)	2.686		P(2)	2.728		As(1)	2.611
	Tc(4)	2.972		Tc(3)	2.972		Mo(2)	2.953
	Tc(4)	3.012		Tc(3)	3.012		Mo(2)	3.234
	Tc(3)	2.999		Tc(4)	2.937		Mo(2)	2.953
	Tc(2)	2.964		Tc(1)	3.013		Mo(1)	3.258
	Tc(4)	3.254		Tc(3)	3.254		Mo(2)	3.234
P(1):	Tc(2)	2.414	P(2):	Tc(1)	2.415	As(1):	Mo(1)	2.574
	Tc(4)	2.434		Tc(3)	2.389		Mo(2)	2.531
	Tc(3)	2.428		Tc(4)	2.392		Mo(2)	2.531
	Tc(3)	2.686		Tc(4)	2.728		Mo(2)	2.611
	P(1)	2.398		P(2)	2.366		As(1)	2.964
P(3):	Tc(1)	2.337	P(4):	Tc(2)	2.423	As(2):	Mo(1)	2.512
	Tc(2)	2.340		Tc(1)	2.416		Mo(1)	2.512
	Tc(3)	2.289		Tc(4)	2.314		Mo(2)	2.573
	Tc(2)	2.394		Tc(1)	2.363		Mo(1)	2.546
P(5):	Tc(2)	2.370	P(6):	Tc(1)	2.446	As(3):	Mo(1)	2.551
	Tc(4)	2.389		Tc(3)	2.431		Mo(2)	2.576
	Tc(1)	2.389		Tc(2)	2.424		Mo(1)	2.551
	Tc(3)	2.420		Tc(4)	2.412		Mo(2)	2.576
	P(6)	2.223		P(5)	2.223		As(3)	2.450

[a] The arrangement of the table exactly follows that of Table III in Ref. (*3*) to facilitate comparisons between the distances of Tc_2P_3 and Tc_2As_3 as well as between the previous (*4*) and the present refinement of the Mo_2As_3 structure. The Tc(1) and Tc(2) atoms of Tc_2P_3 correspond to the Mo(1) atom of Mo_2As_3, the Tc(3) and Tc(4) atoms correspond to Mo(2), etc. Standard deviations computed from those of the lattice parameters and the positional parameters of Tc_2P_3 are all less than 0.0015 Å for Tc–Tc distances, and less or equal to 0.003 Å for Tc–P and P–P distances. In Mo_2As_3 they are all less or equal to 0.001 Å.

for intermetallic compounds, and those of phosphides whose structure can be rationalized on the basis of classical two-electron bonds: Tc_2P_3 has 17 near-neighbor interactions per formula unit which would require 34 valence electrons to saturate two-electron bonds, while there are only 29 valence electrons available. Thus we had concluded earlier (*3*) that most near-neighbor interactions in Tc_2As_3 will come close to classical two-electron bonds, but some bonds, especially also the Tc–As bonds of 2.62 and 2.71 Å, will have bond orders of less than one. It is interesting now that the bonds in Tc_2P_3 corresponding to those weak bonds in Tc_2As_3 are actually longer in Tc_2P_3 (2.69 and 2.73 Å) than in Tc_2As_3.

Thus we note a tendency toward more localized bonding in Tc_2P_3 as compared to Tc_2As_3. If the two weak Tc–P interactions of 2.69 and 2.73 Å are regarded as no bonding interactions we would need only 32 (instead of the previous count of 34) electrons to saturate all short near-neighbor interactions; still too many as compared to the 29 valence electrons available per formula unit, and we expect metallic conductivity. The tendency for more delocalized bonding in going from the light to the heavier main group elements as expressed in a decreasing band gap is well known for isotypic diamond, silicon, and germanium. In going from Tc_2P_3 to Tc_2As_3 we observe this tendency with a gradual change of structure.

The smaller size of the P atoms renders possible stronger Tc–Tc interactions: the four short Tc–Tc bonds of every Tc atom are shortened from an average of 3.020 Å in the Tc_2As_3 to 2.948 Å in Tc_2P_3. The P(5)–P(6) bond length of 2.223 Å corresponds to the bonding interactions in the various modifications of elemental phosphorus (*11*). This bond was already short in Tc_2As_3 (2.447 Å). The other P–P interactions of 2.366 and 2.398 Å are weaker; however, they are stronger in Tc_2P_3 than the corresponding As–As bonds in Tc_2As_3 (2.649 and 2.741 Å): The differences in bond lengths (0.283 and 0.343 Å) are greater than what would be expected from the smaller size of the P atoms (2×0.112 Å as calculated from the average lengths of 2.392 Å for the Tc–P and 2.504 Å for the Tc–As bonds). This again corresponds to increased localization of bonding electrons in Tc_2P_3.

The structure of Tc_2P_3 is a superstructure of Mo_2As_3. It arises through differences in metal–metal bonding (Fig. 3) as was discussed before for Tc_2As_3 (*3*). In Tc_2P_3 the deviations of the Tc atoms from the mirror plane of the Mo_2As_3 type subcell amount to

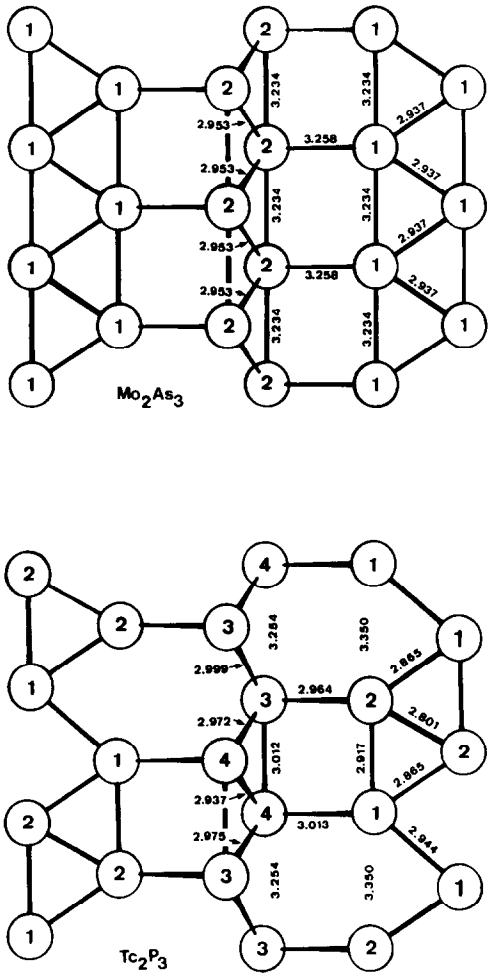

FIG. 3. Metal–metal bonding in Mo_2As_3 and Tc_2P_3. The projections are along the c direction of the monoclinic cell and subcell, respectively, with the [010] direction of Mo_2As_3 and the [100] direction of Tc_2P_3 parallel to the vertical direction of the drawing. The distances are in Å units; large numbers indicate the atom designations.

0.108, 0.108, 0.055, and 0.061 Å for the Tc(1), Tc(2), Tc(3), and Tc(4) atoms, respectively. For the P atoms these deviations are much smaller. They vary between 0.003 Å for P(2) and 0.013 Å for the P(3) atom.[1]

The superstructure in Tc_2P_3 is less pronounced than in Tc_2As_3. This can be expressed quantitatively by a comparison of the metal–metal bond lengths along that translation period which is doubled in the Tc_2As_3 type structure, the direction perpendicular to the mirror plane of the $C2/m$ subcell, which corresponds to the a direction of the Tc_2As_3 structure and to the b direction of the Mo_2As_3 type subcell. In Mo_2As_3 these bonds are all equal and correspond to the short translation period (3.234 Å). In Tc_2As_3 short (2.982 and 3.037 Å) and long (3.594 and 3.538 Å) Tc–Tc distances alternate in that direction. In Tc_2P_3 these differences between short (2.917 and 3.012 Å) and long (3.350 and 3.254 Å) Tc–Tc distances are less pronounced.

Our refinement of the structure of Mo_2As_3 from single-crystal diffractometer data fully confirms the previous structure determination from single-crystal film data (*4*). Although the present structure refinement is more accurate, none of the interatomic distances of the present investigation differs by more than 0.012 Å from those of the previous investigation.

In the remainder of this paper we want to discuss the potential displacive phase transition of Tc_2P_3 and associated phenomena like twinning and anisotropic thermal parameters.

The deviations of the Tc_2P_3 structure from the monoclinic subcell are very small and we assume that upon heating triclinic Tc_2P_3 transforms to the monoclinic Mo_2As_3 structure. Since the crystals were prepared at high temperature we can also assume that they actually grew in the monoclinic high-temperature form and upon cooling transformed to the triclinic low-temperature modification. This transformation lowers the point symmetry from $2/m$ to $\bar{1}$ and in addition also the translational symmetry is lowered by doubling the b axis of the monoclinic cell. Thus, both twin domains and antiphase domains can be expected in the low-temperature form (*12*).

The lattice constants of the monoclinic high-temperature form can be assumed to

[1] These values are readily calculated by transforming the atomic coordinates of the triclinic cell to those of the monoclinic subcell.

be similar to the dimensions of the monoclinic subcell of the triclinic cell determined at room temperature. The powder pattern of Tc_2P_3 actually corresponds to that of the monoclinic subcell (if one disregards the three very weak superstructure reflections). The subcell reflections do not show any line splitting or line broadening due to potential triclinic distortions of the lattice. Therefore the triclinic cell determined from the powder pattern corresponds exactly (apart from the doubling of one translation period) to that of the monoclinic subcell with monoclinic angles $\alpha = \gamma = 90°$ although these angles are allowed to deviate from 90° because they are no longer fixed by symmetry. The lattice constants of the monoclinic subcell determined from the refinement of the single-crystal diffractometer data are less accurate because of systematic errors due to absorption. However, the angles $\alpha = 89.99(1)°$ and $\gamma = 90.03(1)°$ of the monoclinic subcell obtained this way were also very close to 90°.

The twinning described in the experimental section does not seem to be related to the phase transition. In the precession photographs of the reciprocal lattices of the two twin orientations the monoclinic subcells interpenetrate each other in a way which can be ascribed to growth twins. In contrast, if the twinning were due to the phase transition, the two reciprocal lattices should have a *common* monoclinic subcell. Since the distortions of the monoclinic subcell in the triclinic low-temperature form are negligible, the potential twinning due to the reduction in symmetry during the phase transition might be difficult to detect. We have not done any specific experiments (e.g., recording back reflection Weissenberg diffraction patterns or searching for superstructure diffraction signals in the other twin orientation) to search for this twinning.

In this context the anisotropic thermal parameters of Tc_2P_3 are of interest. For almost all atoms the thermal amplitudes are greatest in the *a* direction of the triclinic cell (Table IV). In our experience such a behavior can be ascribed to insufficiently correcting for absorption. In the present case, however, this result may be associated with the potential displacive phase transition of Tc_2P_3.

As discussed above, the deviations from the mirror plane of the monoclinic subcell occur along the *a* direction of the triclinic cell and are greatest for the Tc atoms. In our structure refinement the ratios U_{11}/U_{22} and U_{11}/U_{33} are greatest for the Tc(1) ($U_{11}/U_{22} = 2.25$; $U_{11}/U_{33} = 2.45$) and Tc(2) atom ($U_{11}/U_{22} = 2.35$; $U_{11}/U_{33} = 2.16$). These two atoms have the greatest displacements from the monoclinic subcell. The Tc(3) and Tc(4) atoms have smaller displacements and also smaller U_{11}/U_{22} and U_{11}/U_{33} ratios (2.16; 1.95; 1.68; 1.83 in the corresponding sequence). The displacements of the P atoms are all much smaller and so are their U_{11}/U_{22} (between 0.69 and 1.62) and U_{11}/U_{33} (between 1.06 and 1.38) ratios.[2] Such a correlation between the displacements from a higher symmetry structure and the (apparent) thermal parameters could have been caused by the presence of a small twin domain (with opposite atomic displacements from the high-temperature form) in the "single" crystal used for the collection of the intensity data (assuming that the reciprocal subcells of the two twin domains coincide). If this had been the case, the atomic displacements would be slightly larger than what can be calculated from the potential parameters of the present refinement of the Tc_2P_3 structure.

It is, however, also reasonable to take the anisotropic thermal parameters at their face value, assuming that they are the result of the refinement of data obtained from a

[2] The refinement of the isotypic Tc_2As_3 structure with anisotropic thermal parameters resulted also in relatively large thermal amplitudes U_{11} for the Tc atoms (*3, 13*), although not quite as pronounced as in the present case.

single domain crystal. In the "soft-mode" model for displacive phase transitions (*14*) large thermal amplitudes are expected in the high-temperature form for those atoms which undergo the greatest atomic displacements during the phase transition, and the thermal amplitudes are greatest for the directions of the atomic displacements during the phase transitions. One can assume similar large thermal amplitudes in the low-temperature form along those directions, which lead to the high-temperature form. This was actually observed in the low-temperature modification of β-$Gd_2(MoO_4)_3$ (*15*) and may also be true for triclinic Tc_2P_3. A high-temperature diffraction study of Tc_2P_3 would certainly be of great interest.

Acknowledgments

Thanks are due to Dr. R. Rühl for a Guinier powder pattern and for several crystals of Tc_2P_3. We also want to thank Dr. M. H. Möller for the collection of the four-circle diffractometer data. This work was supported by the Deutsche Forschungsgemeinschaft and the Fonds der Chemischen Industrie.

References

1. R. Rühl, W. Jeitschko, and K. Schwochau, *J. Solid State Chem.* **44,** 134 (1982).
2. R. Rühl and W. Jeitschko, *Acta Crystallogr. Sect. B* **38,** 2784 (1982).
3. W. Jeitschko and L. H. Dietrich, *J. Solid State Chem.* **57,** 59 (1985).
4. P. Jensen, A. Kjekshus, and T. Skansen, *Acta Chem. Scand.* **20,** 1003 (1966).
5. K. Yvon, W. Jeitschko, and E. Parthé, *J. Appl. Crystallogr.* **10,** 73, (1977).
6. D. T. Cromer and J. B. Mann, *Acta Crystallogr. Sect. A* **24,** 321 (1968).
7. D. T. Cromer and D. Liberman, *J. Chem. Phys.* **53,** 1891 (1970).
8. H. Boller and H. Nowotny, *Monatsh. Chem.* **95,** 1272 (1964).
9. J. B. Taylor, L. D. Calvert, and M. R. Hunt, *Can. J. Chem.* **43,** 3045 (1965).
10. P. Jensen, A. Kjekshus, and T. Skansen, *Acta Chem. Scan.* **20,** 403 (1966).
11. J. Donohue, "The Structures of the Elements," Wiley, New York, 1974.
12. H. Wondratschek and W. Jeitschko, *Acta Crystallogr. Sect. A* **32,** 664 (1976).
13. W. Jeitschko and L. H. Dietrich, unpublished results.
14. W. Cochran, *Adv. Phys.* **18,** 157 (1969).
15. W. Jeitschko, *Acta Crystallogr. Sect. B* **28,** 60 (1972).